ISSN 1070-3632, Russian Journal of General Chemistry, 2011, Vol. 81, No. 6, pp. 1392–1406. © Pleiades Publishing, Ltd., 2011.
Original Russian Text © O.A. Golovanova, O.V. Frank-Kamenetskaya, Yu.O. Punin, 2010, published in Rossiiskii Khimicheskii Zhurnal, 2010, Vol. 54, No. 2, pp. 124–136.

Specific Features of Pathogenic Mineral Formation in the Human Body

O. A. Golovanova[a], O. V. Frank-Kamenetskaya[b], and Yu. O. Punin[b]

[a] *Dostoevsky Omsk State University, Omsk, Russia*

[b] *St. Petersburg State University, Universitetskaya nab. 79, St. Petersburg, 199034 Russia*
e-mail: Golovanova2000@mail.ru

Received January 10, 2010

Abstract—Key relationships in pathogenic mineral formation within the human body were summarized. It was shown that pathogenic organomineral aggregates in human body are formed in complex multicomponent media containing organic and inorganic components. In the course of lithogenesis, the composition of biological fluid undergoes major changes. Phase formation in human urine and oral fluid in the initial stages leads to emergence of less thermodynamically stable phases, i.e., is kinetically controlled. Amino acids, as well as a number of inorganic impurities, are actively involved in crystallization of the main phases of renal calculi.

DOI: 10.1134/S1070363211060442

INTRODUCTION

Minerals constitute an essential element of human bioecology. Biomineral formation in human body belongs to the scope of biological mineralogy, a new scientific direction which, in terms of the research objects and methods, is closely related to chemistry, mineralogy, and physics. Biomineralogical studies are focused on structures formed from the mineral and organic constituents that emerged in biosphere and were created in a living organism with its participation or resulted from substitution of dead organic matter for mineral matter. The biominerals that were formed in living organisms are subdivided into physiogenic (essential for physiological processes in humans) and pathogenic groups. Being part of various organs, the former perform various functions, and the latter result from malfunction of the whole body or of its individual organ.

From a genetic viewpoint, pathogenic aggregates, in particular, urinary, biliary, dental, and salivary calculi, and some other, are treated as body "diseases." These aggregates are variable in composition. Difficulties encountered in studying pathogenic minerals are associated above all with the complex material and elemental composition of the calculi which are essentially organomineral aggregates (OMAs) comprising the very difficult to separate mineral (often very poorly crystallized) and organic components. Also, formation and growth of crystalline phases within the calculi involve complex interactions of the living and inert matter, whose mechanisms are understood inadequately and are the subject of debate at the present time.

In recent years there has been increasing interest in studies of pathogenic minerals due to growing incidence of diseases and deepening environmental degradation around the world, which factors belong to those most strongly contributing to emergence of pathogenic biomineral formations. Gaining insight into the genesis of urinary, biliary, and other calculi in human body requires detailed studies of their composition by modern instrumental techniques, and revealing the specific features of formation and growth of crystalline phases therein, an active use of theoretical and experimental modeling methods. Studies into the composition and structure of pathogenic biominerals are currently under way in many research centers both in Russia [1–9] and abroad [10–19], but many relevant issues still remain to be elucidated. Summarization and critical analysis of the accumulated knowledge on the material composition and hypotheses on formation of pathogenic aggregates in human body have revealed the need in clarification, systematization, and reconsideration of the available factual material. The interpretation of the mechanisms

of lithiasis in human body, at the level of speculations, is the subject of much discussion in literature.

Here, we studied the pathogenic mineral formation in human body via detailed examination of the major pathogenic organomineral aggregates (urinary, biliary, dental, and salivary calculi) and their corresponding stone-forming media. We used a collection of calculi removed for health purposes during surgical treatment of patients in Omsk and St. Petersburg, which consisted of uroliths (241), choleliths (185), dentoliths (69), and salivoliths (10). During our experiments we developed and tested techniques for extraction separation of the mineral and organic components of organomineral composites of any nature and also selected and adapted the complementary methods to be used for studying the pathogenic aggregates in human body. Also, we developed a thermodynamic calculational model of phase formation for poorly soluble compounds in biological fluid prototypes, improved the synthesis methods for the main minerals of renal calculi (whewellite and apatite), and adjusted methods for studying the crystallization of calcium oxalate monohydrate and hydroxyapatite.

Our studies on pathogenic mineral formation in human body showed that a transition to the pathogenic state causes the concentration of the major inorganic components in biological fluids to increase, whereas the content of protein and other organic compounds may both increase (bile) and decrease (mixed saliva). Lithogenesis causes substantial, often periodic, alterations in the composition of biological fluids, as seen from a multiphase, microheterogeneous, and zonal nature of calculi and the variability of the composition, observed for most of pathogenic biominerals. Below, the above-mentioned points will be instantiated by specific examples.

Bole as a Stone-Forming Medium

The bile samples collected during surgery from patients in Omsk region were analyzed for the content of the major organic components. Among them, the main bile component, bile acids (cholesterol stabilizers) was detected in subnormal, normal, and supernormal concentrations for 25, 12.5%, and 62.5% of the samples, respectively. The concentrations of cholesterol, phospholipids, and triglycerides were above the norm in all the samples (for cholesterol it was 11 times the normal value, on the average); subnormal and supernormal bilirubin content was revealed in 18.7% and 81.3% of the samples, respectively. Thus, the composition of pathogenic bile is off the norm; in most cases the content of the major organic components is supernormal.

Based on the bile composition data obtained, we calculated by different procedures the lithogenicity indices (LIs) which measure the coagulation stability of bile in order to validate the lithogenic properties of the bile analyzed. Abnormal LI values that were revealed for all the samples in all the cases confirmed the pathogenic properties of the bile analyzed.

As part of assessing the protein content in the tested bile samples we estimated the total nitrogen content at 1.50–1.80 wt %, which is nearly 3 times the nitrogen content in healthy bile (0.48 wt %). Enhanced levels of total nitrogen may be associated with increases in the content of not only amino acids but also of nitrogen-containing organic compounds, bilirubin and phospholipids, observed for bile in pathology.

Increased levels were also characteristic for most of the inorganic components of bile in pathology. Specifically, the weight fractions of sodium, phosphorus and potassium, calcium, and magnesium exceeded the normal levels by the factor of 1.2, 1.5, 2.5, and 4.5, respectively; the iron content was 3.5 times lower that the normal level. Calcium cations are known to perform the cementing function in cholesterol nucleation and to be precipitated from bile as carbonates, palmitates, and phosphates. Thus, deviations in the elemental and material compositions of bile in pathology are evidently responsible for degradation of its colloidal structure, thereby promoting cholesterol coagulation and formation of calculi.

The major mineral component of choleliths is cholesterol which, accordingly, should be removed from the sample so that other constituents of biliary calculi can be detected. To this end we used the stepwise extraction separation technique with respect to components of biliary calculi in the samples [20] and detected, along with anhydrous cholesterol $C_{27}H_{46}O$, the following additional phases: calcium carbonate $CaCO_3$ (vaterite, aragonite, and calcite), calcium phosphate whitlockite $Ca_3(PO_4)_2$, and organic compounds: bilirubin ($C_{33}H_{36}O_6N_4$) and sodium salt of bile acid ($C_{21}H_{37}$=$CONHCH_2COONa$). Two “black calculi” contained negligible amounts of cholesterol and were comprised of bilirubin and calcium palmitate $(C_{15}H_{31}COO)_2Ca$, which means that these are pigment calculi. A zonal-layered structure characteristic of biliary calculi (Fig. 1) is most often due to variations in

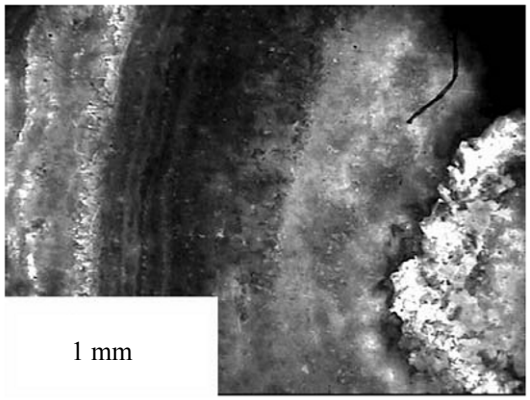

Fig. 1. Zonal-layered structure of a cholesterol calculus.

the phase composition within a single dental plaque liquid. The crust consists predominantly of cholesterol with a minor vaterite impurity; cholesterol, aragonite, and vaterite appear in the middle zone; and the central part of the biliary calculus consists of cholesterol with aragonite traces. The layerwise distribution of the phases is indicative of changes in the physicochemical characteristics of the stone-forming medium.

Over 36 elements were identified in the composition of the examined biliary calculi in proportions ranging from 5.10 to 2 wt %. The percentage of the elements decreases along the following series: Ca, K, Mn, Fe, Cu, Pb, Ti, Zn, V, Ni, Bi, Cr, Hg; the calcium and potassium content is 95 and >3 wt %, respectively; and chromium and mercury account for ~0.02 wt %. An increase in the calcium content, observed for bile in pathology, contributes to formation of choleliths containing calcium carbonates and calcium bilirubinate, the latter being the main phase of pigment calculi. Based on the manganese, iron, and copper concentrations determined, the entire collection can be divided into three groups of samples: Fe > Cu > Mn; Mn > Fe> Cu; and Cu > Fe > Mn. Also, for individual biliary calculi we revealed sharply increased average concentrations of some elements: The lead, mercury, copper, and iron content exceeded the norm by the factor of 50, 12, 290, 59, respectively, which findings may be associated with the environmental situation specific for Omsk region [21].

Table 1. Occurrence rates for mineral associations of uroliths in St. Petersburg and Omsk

Mineral associations	Relative occurrence rate, %	
	St. Petersburg	Omsk
Whewellite + weddellite	28.3	11.5
Whewellite + hydroxyapatite	3.3	19.4
Whewellite + weddellite + hydroxyapatite	5.0	15.8
Whewellite +uric acid (anhydrous)	1.7	12.7
Hydroxyapatite + struvite	8.3	5.5
Uric acid (anhydrous)	3.3	3.9
Brushite + whitlockite + hydroxyapatite	1.7	–
Carbonate apatite + whewellite + weddellite + uric acid (anhydrous)	Not detected	0.6
Weddellite + whewellite + uric acid (anhydrous) + ammonium urate	–	0.6
Uric acid dihydrate	–	0.6
Whewellite + weddellite + struvite + carbonate apatite	–	2.4
Whewellite + struvite	–	0.6
Whewellite + struvite + whitlockite	–	0.6
Struvite + whitlockite	–	1.2
Whewellite + amorphous calcium phosphate	–	1.2
Carbonate apatite + whitlockite	–	0.6
Whewellite + uric acid dihydrate	–	0.6

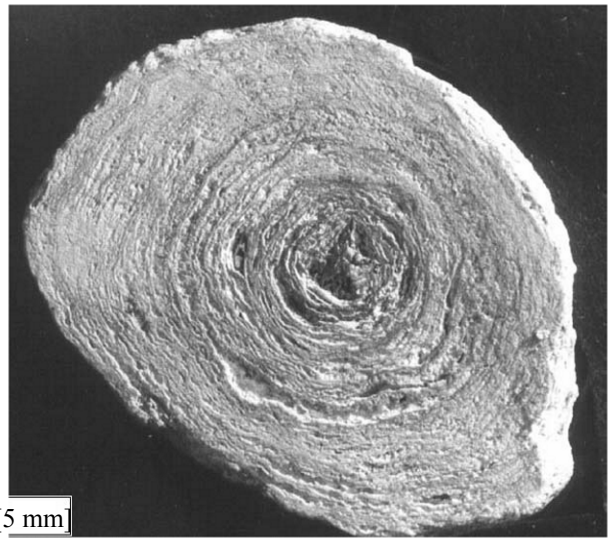

Fig. 2. Layered structure of a phosphate-oxalate renal calculus. Magnification ×1.5.

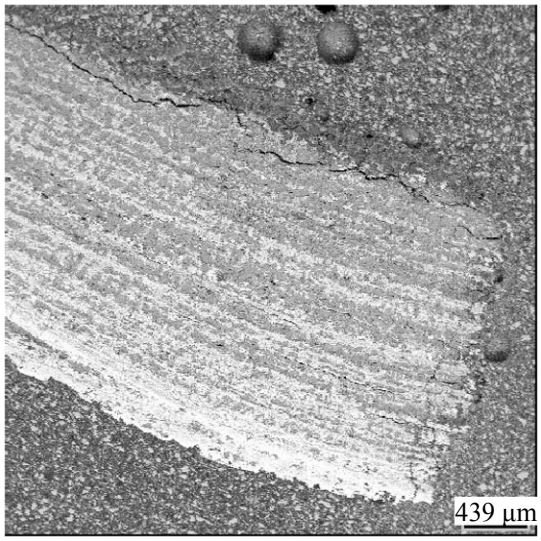

Fig. 3. Zonal distribution of (dark layers) struvite and (white layers) apatite under an electron microscope.

Urine as a Stone-Forming Medium

Among over twenty inorganic and organic compounds identified in healthy human urine, pathological components are glucose, protein, ketone bodies, and blood. Urolithiasis in physiological media leads to increased levels of inorganic phosphorus (>75 mmol l^{-1}), total calcium (>7 mmol l^{-1}), magnesium (> 5 mmol l^{-1}), oxalic acid (>0.25 mmol l^{-1}), and uric acid (>4 mmol l^{-1}). Healthy human urine contains protein traces undetectable by conventional qualitative analysis techniques. Renal and some other diseases cause an increase in the amount of proteins excreted in urine. The daily average healthy urine pH falls between 5.5 and 6.5. Oxalic, uratic, and phosphatic lithiasis involves pH variation throughout the day within 4.8–7.0, 4.5–5.8, and 6.0–7.7, respectively [5]. Thus, urine is a complex multicomponent solution which, in terms of its chemical composition and acidity, most strongly contributes to pathogenic mineral formation in the urinary system.

By now, 29 minerals were identified in uroliths, most of which are calcium salts. Among the eleven compounds detected in the calculi from the examined collection, the most frequently occurring salts are oxalates: whewellite $CaC_2O_4 \cdot (1 + x)H_2O$ ($x \leq 0.07$) and weddellite $CaC_2O_4 \cdot (2 + x)H_2O$, ($x \sim 0.13$—$0.37$); phosphates: struvite $MgNH_4PO_4 \cdot 6H_2O$, hydroxyapatite $Ca_5(PO_4)_3(OH)$, brushite $CaHPO_4 \cdot 2H_2O$, and whitlockite $Ca_3(PO_4)_2$; urates: uricite $C_5H_4N_4O_3$, uric acid dihydrate $C_5H_4N_4O_3 \cdot 2H_2O$, and ammonium urate $C_5H_2O_3N_4(NH_4)_2$. Quartz SiO_2 was detected in 5% of the samples of renal calculi solely; one of the calculi contained, along with quartz, calcium silicate hatrurite Ca_3SiO_5, which was detected for the first time. The occurrence rates of minerals in uroliths from different regions are variable. The steadily dominating oxalate calculi (45–75%) are followed by those from phosphate (20–40%) and urate (10–20%) group. Table 1 presents the typical parageneses of the basic mineral components of uroliths and their occurrence rates for the collection examined by us.

The uroliths that we examined have for the most part a layered, often fine-zonal structure comprised of alternating mineral and organic layers and layers of different mineral composition. Layering can be observed at different examination levels during visual examination of sections of large calculi (Fig. 2) and in electron images of individual segments of the samples (Fig. 3).

We identified for the first time the main types of localization for organic protein substances: core (at the aggregate center), interlayer-type (concentric and radial interlayers), and diffuse (inclusions in mineral crystals). All these localization types commonly coexist in uroliths, with one of the types being markedly predominant. Scanning electron microscopic examinations revealed microheterogeneity in virtually all the uroliths examined. In the oxalate and struvite calculi (monomineral, according to X-ray phase analysis data) we revealed apatite grains (4–5 μm); the

Table 2. Comparative characterization of the electrolyte composition of the oral fluid for Omsk residents[a]

Oral fluid composition	Patient group			
	control	administering medicines	subjected to computer exposures	vulnerable to caries
pH	6.80±0.11	7.04±0.02	6.75±0.35	6.59±0.09
Na^+, g l^{-1}	0.30±0.04	0.38±0.08	0.31±0.12	0.32±0.06
K^+, g l^{-1}	0.72±0.05	1.15±0.03	0.77±0.25	1.08±0.32
Total calcium content, g l^{-1}	0.051±0.004	0.057±0.005	0.049±0.013	0.05±0.01
Phosphorus content, g l^{-1}	0.16±0.01	0.20±0.02	0.15±0.05	0.19±0.05
Protein content, mg ml^{-1}	1.73±0.24	1.33±0.06	1.69±0.07	1.68±0.75

[a] The confidence intervals correspond to $P = 0.95$.

phosphate and urate calculi comprised individual small whewellite crystals (150–200 μm in size). The data on the variations in the crystal lattice parameters and local microanalysis data suggest a variable nonstoichiometric composition for the oxalates and phosphates in the renal calculi, which is indicative of nonequilibrium and nonstationary conditions of their formation.

Nonstoichiometric composition of calcium oxalates (whewellite and weddellite) stems from variability of the water content therein. Variations in the composition of struvites and apatites are associated with isomorphic substitutions for all the crystallographic sites. The main impurities in struvites from renal calculi, wt %, include Ca (0.36–1.89), Na (up to 0.13), K (0.28–0.70), and S (0.5–0.8), and those in apatite from renal calculi, wt %, Na, Mg (0.5–0.8), K (0.3–0.4), S (0.5–0.8), and Cl (0.07–0.30). The nonstoichiometry of struvite and apatite is associated with a variable content of vacancies at the Mg and Ca sites, respectively.

Cluster analysis showed that the oxalate, phosphate, and urate renal calculi differ in the content of Ca, P, Mg, Na, K, S, F (> 0.1 wt %), as well as of Sr, Zn, Ba, Cu, Br, Pb, Sb, Zr, Rb (<0.1 wt %). As to mixed-composition (phosphate-oxalate and urate-oxalate) calculi, this differentiation is vague. A maximal number of trace elements (F, K, Sr, Zn, Ba, Zr, Sb, Rb) is more characteristic for the phosphate group, which fact can be explained by their isomorphic incorporation into the crystal structures of phosphates, above all, of hydroxyapatite.

Oral Fluid as a Stone-Forming Medium

We analyzed oral fluid (mixed saliva) for the content of its major components in 4 groups of Omsk residents (a total of 250). Table 2 summarizes the results, which suggests that dentoliths were present in the oral cavity of patients from all the tested groups except for the control group. A significant change (relative to the control group) in the saliva parameters was revealed in persons administering medicines and those vulnerable to dental caries. Their oral fluid contained enhanced concentrations of the potassium and sodium ions and decreased amounts of protein and inorganic phosphorus, and its pH value was off the norm.

Fifteen amino acids with the total content of 0.34 wt % on the average (subnormal value) were identified in the organic component of oral fluid in the Omsk residents tested. Moreover, in all the persons whose oral cavities contained dentoliths there were enhanced (~0.5 mg l^{-1}) levels of some trace elements (Fe, Mn, Ni, Al, Zn, and Cu). We revealed different microcrystallization patterns for healthy human saliva (control group) and saliva of the persons subjected to prolonged exposures to computers, and for the latter group we proposed a procedure for assessment of the oral cavity condition [22].

The dentoliths and salivoliths examined by us contained various calcium phosphates: apatite, brushite, octacalcium phosphate $Ca_8H_2(PO_4)_6 \cdot 5H_2O$, and whitlockite. The most common mineral is apatite which is known to be the sole mineral component of hard dental tissues (enamel, dentin). Thus, pathogenic formations appearing in the oral cavity (dentoliths and salivoliths) are characterized by more diversified mineral composition than are physiogenic ones.

Variations in the crystal lattice parameters of apatites in salivoliths and dentoliths are also associated

with isomorphism which is broadly manifested in all the crystallographic sites. The main impurities in apatites from salivary and dental calculi include, wt %, Na (0.4–1.0), Mg (0.5–3.7), K (0.02–0.30), S (0.4–1.0), and Cl (0.02–0.20).

The range of variation of the lattice parameters for apatites in salivary and dental calculi is broader compared to that for apatites of hard dental tissues, though significantly narrower than that for the apatites from uroliths. Consequently, the chemical composition and pH of oral fluid varies over a narrower range compared to urine. Different variation ranges for the crystal lattice parameters of physiogenic and pathogenic bioapatites suggest the following: Formation of hard dental tissue is completely controlled by human body, and formation of OMAs is associated with abnormal changes in parameters of the stone-forming medium. Also, dentoliths and salivoliths are characterized by a concentric layered structure, with inorganic layers typically separated by thinner organic layers. Most of the calculi examined by us originated from one nucleus, but there also exist calculi in which the concentric layers are formed around multiple nuclei.

The total content of amino acids in salivoliths and dentoliths significantly exceeds that in pathogenic oral fluid. The trends in variation of the average concentrations, wt %, of the chemical elements for dentoliths (Zn > Fe > Cu > Ni > Mn) are virtually identical to those for oral fluid. This suggests that amino acids that easily form complexes with the respective heavy metals are eliminated from the general circulation of amino acids. This disturbs the bonds linking the calcium ions with protein colloids of saliva, and the liberated calcium ions get bound by the phosphate ions into insoluble calcium phosphates which are the major components of dentoliths and salivoliths.

The results of thermodynamic calculations, as well as of experiments with prototypes of biological fluids and studies of the actual composition of the OMAs, suggest that the pathogenic phase formation in human body is an extremely nonequilibrium process. High occurrence rate revealed for calcium oxalate monohydrate (whewellite) and basic calcium phosphate (apatite) is associated with a high supersaturation of the biological fluid with respect to these phases. The phase formation is more strongly affected by pH of solution than by variation in the initial concentrations of the components. The highest stability of apatite, associated with a broader range of variation of its formation conditions, is responsible for its occurrence in virtually all uroliths, dentoliths, and salivoliths.

To explore the possibility of formation of a poorly soluble compound we used the calculated values of the saturation indices *SI*; the supersaturation *S* in solution with respect to a poorly soluble compound ($M_{p+}A_{q-}$) was calculated by the equations:

$$S = \left[\frac{(a_{M^{m+}})_S^{p+} (a_{A^{a-}})_S^{q-}}{(a_{M^{m+}})_\infty^{p+} (a_{A^{a-}})_\infty^{q-}} \right]^{\frac{1}{p_+ + q_-}} = \left(\frac{IAP}{K_S^0} \right)^{\frac{1}{p_+ + q_-}}, \quad (1)$$

$$SI = \log (S), \quad (2)$$

where *IAP* is the ion activity product.

The stability ranges for poorly soluble phases of uroliths, dentoliths, and salivoliths were determined via calculations using the Gbflow3 program (version 3.1).

The results of the thermodynamic calculations were verified in a series of experiments on phase formation in prototypes of biological fluids (urine, oral fluid, dental plaque fluid). The ionic composition (inorganic macro components), temperature, ionic strength, and pH of the tested solutions corresponded to those of the respective media in human body. The phase composition of the synthesized material was determined by X-ray phase analysis, IR spectroscopy, and chemical analysis methods.

Uroliths

As follows from the supersaturation indices calculated by us, formation of the following phases is thermodynamically probable in the solutions examined: brushite $CaHPO_4 \cdot 2H_2O$; whitlockite $Ca_3(PO_4)_2$; hydroxyapatite $Ca_{10}(PO_4)_6(OH)_2$; whewellite $CaC_2O_4 \cdot H_2O$; weddellite $CaC_2O_4 \cdot 2H_2O$; caoxite $CaC_2O_4 \cdot 3H_2O$; calcite $CaCO_3$; newburyte $MgHPO_4 \cdot 3H_2O$; and struvite $MgNH_4PO_4 \cdot 6H_2O$.

Out of the above-listed compounds, only calcium oxalates with different degrees of hydration can be formed throughout the pH range examined (4.5–8.0), with $CaC_2O_4 \cdot H_2O$ (whewellite) being the most stable modification, as confirmed by the experimental data on crystallization of oxalates at pH 4.8–7.0. In solutions with pH 4.5–5.6 the precipitation of poorly soluble

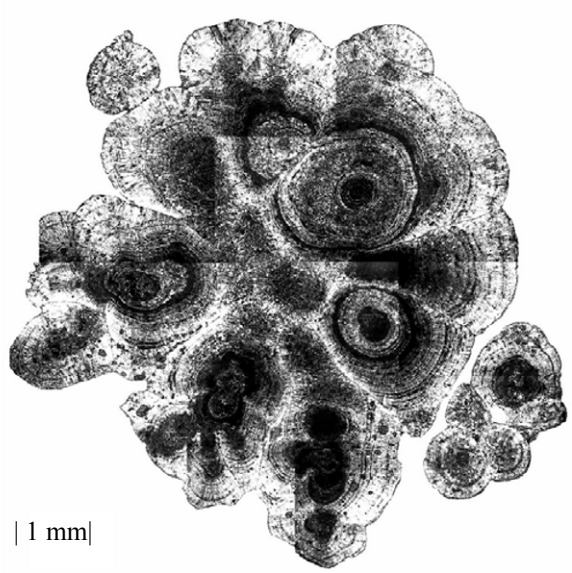

Fig. 4. Thin-section image of an oxalate calculus: whewellite spherulites.

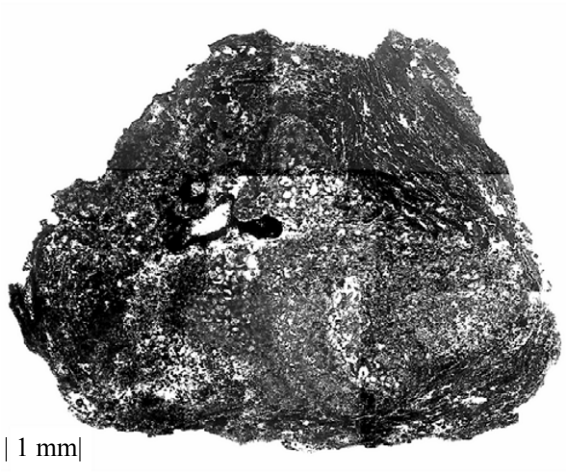

Fig. 5. Thin-section image of a struvite-apatite urolith.

calcium and magnesium phosphates is thermodynamically impossible. This fact is confirmed by the experimental data indicating that hydroxyapatite is formed in weakly alkaline (pH 6.5–7.8) solution. Comparison of the supersaturation indices calculated for calcium phosphates of different stoichiometries (at pH 5.2–8.0) revealed the highest degree of supersaturation for hydroxyapatite.

At pH < 6.5 the SI for the calcium phosphates examined decreases as $CaHPO_4 \cdot 2H_2O$ > β-$Ca_3(PO_4)_2$ > $Ca_4H(PO_4)_3 \cdot 2.5H_2O$, and at pH > 7.5, as β-$Ca_3(PO_4)_2$ > $Ca_4H(PO_4)_3 \cdot 2.5H_2O$ > $CaHPO_4 \cdot 2H_2O$.

Magnesium phosphates (e.g., struvite) may be formed in the examined solutions at pH > 6.0 solely. A model experiment revealed formation of trace amounts of hydroxyapatite in nearly all the tests, with brushite and amorphous calcium phosphate being the main phases in the precipitates isolated. Thermodynamic calculations showed that, under the experimental conditions, these are metastable phases, i.e., that equilibrium with respect to hydroxyapatite was not established. On the whole, our results adequately explain a widespread occurrence of hydroxyapatite (though often in minor amounts) in virtually all human renal calculi. Theoretical and experimental modeling data suggest that pH of the solution much more strongly affects the composition of the resulting solid phase than does the variation of the initial concentrations of its components. Our thermodynamic calculations showed that the biological solution is supersaturated with respect to the main phases of renal calculi (whewellite and hydroxyapatite). The fact that only a limited number of people suffer from urolithiasis may be explained by stabilization of the solution by protein compounds and amino acids.

Dentoliths and Salivoliths

The thermodynamic calculations for mixed saliva showed that, at pH < 6.5, the SI for the examined calcium phosphates decreases as $Ca_{10}(PO_4)_6(OH)_2$ > β-$Ca_3(PO_4)_2$ > $CaHPO_4 \cdot 2H_2O$> $Ca_4H(PO_4)_3 \cdot 2.5H_2O$, and at pH > 7, as $Ca_{10}(PO_4)_6(OH)_2$ > β-$Ca_3(PO_4)_2$ > $Ca_4H(PO_4)_3 \cdot 2.5H_2O$ > $CaHPO_4 \cdot 2H_2O$. Similar trends were revealed for dental plaque fluid, with precipitation of dental calculus phases shifted to higher acidities. Under typical conditions of dentolith and salivolith formation, brushite is the thermodynamically nonequilibrium phase with respect to hydroxyapatite. Hence, the emergence of brushite in the initial stage of formation of these OMAs is for the most part kinetically controlled, and its subsequent transformation into hydroxyapatite is due to the fact that the system strives for thermodynamic equilibrium.

In the model experiments we obtained analogs of the following dentolith and salivolith minerals: brushite, struvite, apatite, and X-ray amorphous calcium phosphate. In all the experiments the precipitates were dominated by brushite, and the content of poorly crystallized apatite tended to increase

with increasing pH of solution. Comparison of the thermodynamic calculation and modeling results with the data on the mineral composition of dentoliths and salivoliths shows that brushite, octacalcium phosphate, and whitlockite are metastable phases.

Overall, the thermodynamic calculation and modeling data suggest the decisive importance of nonequilibrium processes in the formation of crystalline phases of uroliths, dentolith, and salivolith, with hydroxyapatite being the most thermodynamically stable phase in these aggregates, which validates a special contribution that it makes to their formation.

In the next stage of our study we determined the relationships in crystallization of the main phases of urinary, biliary, dental, and salivary calculi via analyzing their ontogeny and modeling in prototypes of biological fluids.

Ontogenetic Relationships

The results of examinations of the structural and textural features of pathogenic aggregates suggest their stepwise formation. Many of uroliths, dentolith, and salivolith exhibit growth patterns with breaks; the dissolution of the earlier formed layers is not an infrequent event leading to several zones overlain "unconformably" by the newly emerged layers. An X-ray computed microtomography examination revealed hidden density anomalies, specifically, decreased densities, which are also indicative of alterations of the formation conditions for uroliths, dentoliths, and salivoliths.

On the whole, our findings suggest that lithiasis proceeds under very complex and variable conditions, with the growth of calculi repeatedly alternated by their dissolution. The uroliths from the collection examined by us, which are comprised of whewellite, weddelite, or uricite, typically have a spherulitic (Fig. 4) or dendritic structure.

The spherulite growth occurs via intense splitting of crystals and often leads to spherulites composed of a single mineral. A spherulitic structure of the aggregates is indicative of direct crystallization of the calculus components originating at the initiating nuclei. In this case, crystallization of the metastable phase (weddellite) may be followed by its substitution for whewellite. Thin-sections images are indicative of changes in the substance deposition intensity, with spherulitic aggregates growing under repeated nucleation of spherulites. The growth boundaries at the points of contact of spherulites form a complex system of cavities (cavernous aggregates).

The granular structure of phosphate calculi (uroliths, dentoliths, and salivoliths) suggests that these OMAs are formed primarily via sedimentation and agglomeration of fine-grained or amorphous material (Fig. 5). Being of subordinate importance in the case of interest, crystallization contributes to formation of secondary minerals with higher solubilities (oxalates, struvite, and brushite). Uroliths, typically of the mixed type, have a layered structure comprised of alternating granular and spherulitic aggregates. Such calculi are formed under furthest from equilibrium conditions via two alternating processes of crystallization and sedimentation. The layered structure is better defined in spherulitic than in granular calculi. Overall, the ontogenic relationships revealed for uroliths, salivoliths, and dentoliths are mutually consistent and complementary to the urolith data that were earlier obtained by A.K. Polienko, V.I. Katkova, F.V. Zuzuk, et al.

Biliary calculi are represented primarily by concentric-zonal spherulites having a thin-layered peripheral shell and coarser-zoned core and intermediate segments. Metabolism and the periodic bile secretion promote formation of concentric rings of different colors. The radial, coarse, and fan-like spherulitic structure of cholesterol biliary calculi is indicative of their formation from true solutions. Zonal distribution of the calculus color suggests that the same calculus can be alternately formed from true bile and from colloidal, bilirubinate-enriched bile solution. Presumably, bile in the gallbladder periodically changes from true to colloidal solution state.

Thus, calculi whose mineral component is represented by organic compounds (oxalate and urate uroliths; cholesterol calculi) are characterized by a spherulitic structure and exhibit direct phase growth from supersaturated solutions. Phosphate calculi (phosphate uroliths, dentoliths, and salivoliths) have a granular cryptocrystalline structure and are formed by the sedimentation mechanism.

Let us discuss the results of modeling in prototypes of biological fluids. The synthesis of calcium oxalate monohydrate from aqueous solutions under close to physiological conditions (pH 4.5, 6.0, 7.5; ionic strength 0.3) is unaffected by pH of solution and temperature, as well as by introduction into the system

Table 3. Effect of amino acids on the electrolkinetic properties of hydroxyapatite sol particles. I = 0.3, pH = 6.5, C_{aa} = 0.004 M

Ca/P atomic ratio	Amino acid	Sign of charge of the particles	Electrophoretic mobility, cm	ξ-Potential, mV
1.58±0.01	–	–	2.1×10^{-4}	–28.6
	Glycine (Gly)	+	1.2×10^{-4}	16.3
	Aspartic acid (Asp)	–	1.0×10^{-4}	–22.2
	Glutamic acid (Glu)	–	1.6×10^{-4}	–13.8
	Lysine (Lys)	+	2.1×10^{-4}	28.3
1.65±0.01	–	–	5.9×10^{-5}	–8.0
1.67±0.01	–	+	5.4×10^{-5}	7.4
	Glycine (Gly)	–	8.7×10^{-5}	–11.7
	Aspartic acid (Asp)	–	1.2×10^{-4}	–17.0
	Glutamic acid (Glu)	–	1.2×10^{-4}	–16.5
	Lysine (Lys)	+	5.4×10^{-5}	7.20

Table 4. Dispersion analysis data for the average particle size (D) of the hydroxyapatite synthesized in the presence of amino acids

Amino acid	Ca/P (s.) = 1.58±0.01		Ca/P (s.) = 1.65±0.01		Ca/P (s.) = 1.67±0.01	
	D, μm	Δ[a], %	D, μm	Δ[a], %	D, μm	Δ[a], %
No amino acid addition	17.3	0.0	22.54	0.0	28.35	0.0
Glycine (Gly)	16.94	–2.10	19.32	–14.3	32.10	13.2
Aspartic acid (Asp)	15.62	–9.50	17.49	–22.4	18.20	–35.8
Glutamic acid (Glu)	14.65	–15.3	17.81	–21.0	21.10	–25.6
Lysine (Lys)	12.35	–28.6	16.54	–26.6	21.93	–22.7

[a] Δ, % is the measurement inaccuracy; rms variance Sr = 0.02–0.03.

of inorganic and organic additions typical of physiological fluids [23].

To elucidate how supersaturation affects nucleation of calcium oxalate monohydrate we determined the induction period, i.e., the time taken for the formation of the first crystals in solutions without additions. The induction period is inversely proportional to the nucleation rate which, in turn, is described by an exponential function of supersaturation, whose parameter is represented by the surface energy s at the crystal–solution interface. Based on the slopes of the corresponding plots, the surface energies were estimated at 36.4 and 20.7 kJ m^{-2} for supersaturations of 5–15 and 15–25, respectively. Such patterns in induction period are usually interpreted as being due to a transition from heterogeneous nucleation at low supersaturations to homogeneous nucleation at high supersaturations, with the lower value of the surface energy treated as an "effective value" associated with adhesion of the nucleus on the active site.

The conductometrically followed kinetic curves show a monotonic increase in the degree of completion of whewellite crystallization in time [$\alpha = (C_0 - C_t)/(C_0 - C_s)$, where C_0 is the concentration of the substance in the supersaturated solution, and C_s, its solubility]. The process is gradually decelerated because of decline in supersaturation during crystallization. Character-istically, even at small α values the process occurs to negligible extent. However, with a probability P = 0.95 (in three parallel experiments for each series, α varied from 0.26 to 0.29) we revealed no difference in the end values of the parameter α for different supersaturations (5, 7, 10). Crystallization in different series of experiments terminated at different

supersaturations, which were the higher the higher the initial super-saturation. These relationships can be explained by manifestation of secondary processes (aggregation, recrystallization of the particles, impurity poisoning, etc.), which occur independently of the initial supersaturation. We examined crystallization of calcium oxalate monohydrate in relation to the ionic strength of the medium and found that, at the ionic strength of 0.3 corresponding to that of physiological fluid, crystallization does not occur at supersaturation $\gamma = 7$ and begins only at $\gamma = 10$.

These results are attributable to the fact that the processes occurring in high ionic strengths solutions are strongly affected by electrostatic repulsive forces acting between similar ions, which makes the calcium cations and oxalate anions less capable of chemical interaction and, thereby, of nucleation. Experimental studies of the role played by magnesium cations in crystallization of calcium oxalate monohydrate also revealed their strong inhibitory action. The particle size distribution analysis showed that, upon addition of the magnesium cations with $C = 10^{-3}$ M to solutions with supersaturation $\gamma = 7$, the average crystal size decreased 2.5 times, i.e., the crystal growth was very strongly inhibited. An increase in the magnesium cation concentrations to $C_{Mg} = 10^{-2}$ M (physiological concentration) causes the inhibitory action to enhance; crystallization of whewellite at this supersaturation ($\gamma = 7$) does not occur at all. Formation of crystals of this phase at the physiological concentration of the magnesium cations in solution begins only at supersaturation $\gamma = 20$.

Thus, the magnesium ions exert a much stronger inhibitory effect on the whewellite crystallization than does the ionic strength. Upon adding hydroxyapatite crystals with the size of (4.29±0.06 μm) into a calcium oxalate solution ($\gamma = 7$, pH 6.5) the average size of the calcium oxalate monohydrate crystals significantly increases from 6.38±0.19 to 14.14±0.29 μm. Hence, the hydroxyapatite crystals occurring in solution exert an initiating effect on the crystallization of calcium oxalate monohydrate. Apparently, the apatite crystals act as heterogeneous nucleation sites for whewellite.

Experiments on synthesis of hydroxyapatite from solutions imitating biological fluid (pH 4.5; 6.0; 7.5; ionic strength 0.3) in the presence of oxalate ions (0.23 mM) and of other additions, which are components of biological solutions, showed the following [4]: An increase in the magnesium cation concentration (> 8.2 mM) leads to formation of struvite, and an excess of carbonate ions (> 50 mM), to precipitation of calcite; the oxalate ions and amino acids do not affect the phase composition of the resulting precipitate.

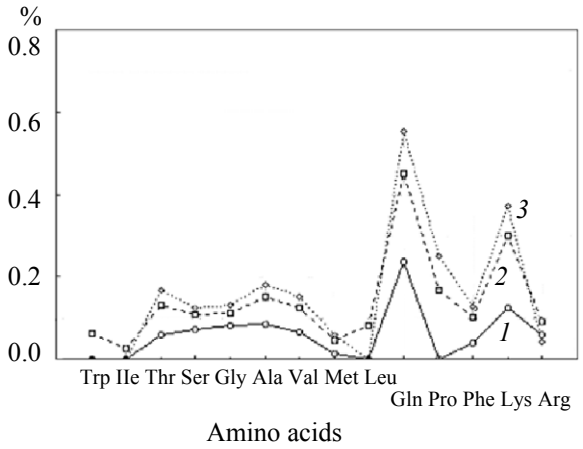

Fig. 6. Average content of amino acids in urinary calculi from different clusters: (*1*) oxalates, (*2*) phosphates, and (*3*) urates.

Studies of the electrokinetic characteristics (sign of the charge, electrophoretic mobility, and ξ-potential) of the synthesized hydroxyapatites showed that the charge and the ξ-potential for the hydroxyapatite particles depend on the stoichiometry (Ca/P atomic ratio): As the Ca/P ratio approaches the stoichiometric value of 1.67, the ξ-potential of the particles tend to shift to positive values (Table 3).

This trend can be explained by incomplete compensation of the charges in nonstoichiometric hydroxyapatites $Ca_{10-x}(PO_4)_{6-x}(HPO_4)_x[OH_{2-x}(H_2O)_x]$. The negative charge of the particle surface may be also

Table 5. Induction period for calcium oxalate monohydrate ($\gamma = 7$) in the presence of amino acids

Amino acid	Concentration, M	Time, s
No amino acid addition	0	663
Glutamic	10^{-5}	578
	10^{-2}	2365
Aspartic	10^{-5}	567
	10^{-2}	1920
Glycine	10^{-5}	55
	10^{-2}	2
Proline	10^{-5}	32

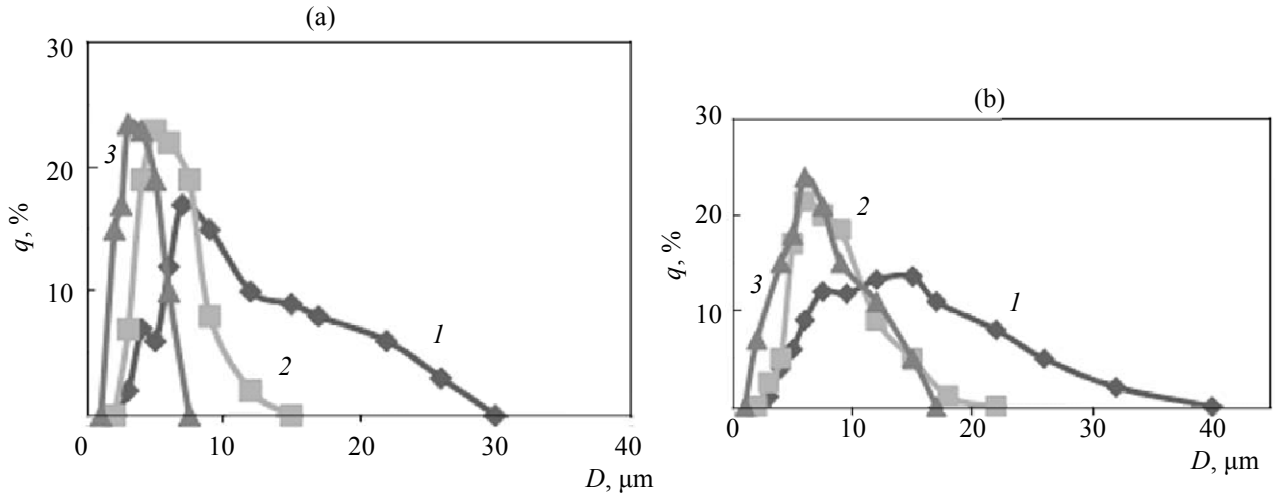

Fig. 7. Volume fraction of calcium oxalate monohydrate crystals q, %, vs. crystal size: Supersaturation γ of (a) 7 and (b) 10. Addition: (*1*) without addition and (*2, 3*) with addition of $C = 10^{-5}$ M of (*2*) aspartic and (*3*) glutamic acid.

associated with partial dissociation in solution of the surface hydrophosphate groups with elimination of a hydrogen ion. A positive charge of the hydroxyapatite particles, characteristic for the stoichiometric Ca/P ratio, can also be explained by incomplete compensation of the positive charge in structures characterized by less pronounced calcium deficiencies. However, this may be due to adsorption on the particle surface of the excessive Ca^{2+} from solution. The latter presumption is consistent with the Fajans–Paneth rule stating that the ions entering into the particle composition are potential-determining ions in micelles existing in solutions.

Table 6. Kinetic characteristics of the calcium oxalate monohydrate crystallization in the presence of the amino acids

Amino acid	Concentration, M	Precipitation rate constant K' at γ = 7
No amino acid addition	0	10^{23}
Glutamic acid	10^{-5}	10^{10}
	10^{-2}	10^{5}
Aspartic acid	10^{-5}	10^{11}
	10^{-2}	10^{7}
Proline	10^{-5}	10^{12}
	10^{-2}	10^{9}
Alanine	10^{-5}	10^{14}
	10^{-2}	10^{10}
Glycine	10^{-5}	10^{13}
	10^{-2}	10^{9}

As shown by dispersion analysis, with increasing Ca/P ratio in the solid phase and, correspondingly, in the initial solution used for the synthesis, the average particle diameter of the hydroxyapatite particles tends to increase (from 17.30 to 28.35 μm). The bimodality of the distribution curve gets more pronounced as the Ca/P ratio is successively increased, which may be associated with a stronger particle aggregation. This finding, in turn, may be attributed to a decrease in the charge of the particles of the resulting sols (Table 4), which is accompanied by a decrease in the electrostatic repulsion forces acting between the particles and by an increase in the degree of their aggregation. Specifically the aggregation of the particles underlies the "sedimentation" mechanism of phosphate lithiasis.

Some researchers point out that the crystallization studies with respect to biominerals are complicated by a large number of factors differently affecting the process occurring in biological systems. Among them, a strong influence is exerted by organic substances [24], in particular, by those of protein nature, which are biological fluid components.

To assess the contribution made by the protein components to pathogenic mineral formation in human body, we elucidated the links existing between the organic and mineral components of the OMAs and examined the crystallization of the major phases of uroliths (whewellite and hydroxyapatite) as influenced by amino acids. Experiments with separation of the

Table 7. Average size of calcium oxalate monohydrate crystals, μm, in crystallization with amino acid added (supesaturation $\gamma = 7$)

Amino acid	Concentration, M	
	10^{-5}	10^{-2}
Glutamic acid	3.88 ± 0.09	<0.03
Aspartic acid	5.08 ± 0.06	<0.03
Glycine	6.11 ± 0.07	3.95 ± 0.05
Alanine	5.52 ± 0.04	4.32 ± 0.06
Proline	5.30 ± 0.07	4.73 ± 0.04
No amino acid addition	10.31 ± 0.07	

protein components by the original technique showed [5] that, depending on the mineral composition of uroliths, the average content in them of water-soluble organic substances containing a peptide bond varies from 1.4 to 3.8 wt %.

The content of amino acids in uroliths with different mineral compositions tends to decrease along the series urate > urate oxalate > phosphate > oxalate phosphate > oxalate. Cluster analysis showed that, based on qualitatively and quantitatively different assemblages of amino acids therein, uroliths can be subdivided into urate, phosphate, and oxalate groups (Fig. 6).

Analyses of amino acids in different pathogenic formations (uroliths, dentoliths, and salivoliths) showed that the content of glutamine and lysine in them exceeds that of other amino acids. These two amino acids are distinguished by the presence in their composition of additional side functional groups (amino groups in lysine, and carboxy residue, in glutamic acid), which allow them to actively participate in OMA formation. This presumption was confirmed by the results of the experiments on the whewellite and apatite crystallization in the presence of amino acids.

Effect of Amino Acids on the Whewellite Crystallization

Our experiments were concerned with amino acids contained in phosphate type renal calculi and urine in relatively high concentrations. We used model solutions for which pH (6.45±0.05), ionic strength (0.3), and concentration of amino acids (0.004 M) were close to those in the urolith-forming medium. Preliminary experiments showed that the concentration of glutamic and aspartic acids affect the mineral formation kinetics.

The nature of amino acid is also essential for the nucleation of calcium oxalate monohydrate. Glycine and proline occurring in solution exert a catalyzing effect on formation of nuclei (Table 5), which is the stronger the higher the amino acid concentration. Such behavior of "short-chain" amino acids can be explained by close geometric sizes of these amino acids and the oxalate ion. In the case of interest, the calcium cations in solution may be involved in the formation of not only calcium oxalate monohydrate but also of chelate complexes with amino acids which, in turn, become crystallization sites.

The kinetic curves show that the degree of completion of calcium oxalate crystallization in time a decreases in the presence of amino acids, specifically, the stronger the higher the concentration of the addition introduced. This fact can be explained by decreases, during crystallization of the poorly soluble compound examined, in the amount of mobile ions and in the total conductivity of the system in proportion to the residual ion concentration and quantity of the resulting precipitate.

In the context of mineralization kinetics studies, of principal interest is the portion of the kinetic curve in which the particles grow in size, while their total number remains unchanged. Therefore, specifically this portion was used for calculating the main kinetic characteristics of crystallization of calcium oxalate monohydrate (Table 6). We found that, when in the concentration of 10^{-6} M, amino acids do not affect the calcium oxalate growth kinetics at supersaturations of 5–7. An increase in the concentrations of amino acids by an order of magnitude to 10^{-5} M causes both the rate constant and order of the precipitation reaction to decrease, and a further increase to 10^{-2} M causes a dramatic decrease in the crystallization rate constant.

The inhibitory effect of the amino acids can be explained by adsorption of their ions on the active sites of crystal growth for whewellite. Considering the data on the zwitterionic form of occurrence of amino acids in aqueous solutions, as well as the ionic nature of calcium oxalate monohydrate, the electrostatic interaction of amino acids with the surface of the synthesized crystals seems to be the most probable option. An increase in the amino acid concentration in solution leads to blocking of a large number of active sites and deceleration of the crystal growth. Of all the amino acids examined by us, glutamic acid affects the whewellite crystal growth most profoundly.

Dispersion analysis (minimal crystal size 0.03 μm) showed that the amino acids differently affect the induction period. At $\gamma = 7$ upon adding 10–5 M proline, glycine, and alanine, the first crystals of calcium oxalate were detected already after <1 min had elapsed since the beginning of the crystallization reaction, and upon adding glutamic acid in the same concentration, after >5 min of the reaction time. In a system without amino acid additions the crystal formation began virtually immediately after the solutions were poured together. For calcium oxalate monohydrate without additions we recorded a broad bimodal distribution curve, which, moreover, tends to broaden with increasing supersaturation (Fig. 7).

The crystal growth during the crystallization probably occurs simultaneously on crystallization sites of several types, which fact is responsible for polymodal distribution curves that we recorded and whose bimodality tends to increase with increasing supersaturation. Amino acid additions cause sharp narrowing of the distribution curves and a decrease in the average size of the crystals. This validates the conclusions concerning the growth of the calcium oxalate monohydrate crystals, which were derived from the kinetic experimental data concerning the inhibitory effect exerted by aspartic and glutamic acids. Moreover, the inhibitory effect of amino acids gets more pronounced at lower supersaturations. Also, under low supersaturation conditions, the average size of the crystals formed in the presence of glutamic acid is smaller than that in the presence of aspartic acid. We found that the inhibitory effect tends to enhance with increasing amino acid concentration (Table 7).

Of special significance for the nucleation and growth of calcium oxalate monohydrate crystals is glutamic acid. A factor specifically affecting the adsorption is pH: With pH increasing to over 6–8 the adsorption effect markedly decreases. Crystallization of calcium oxalate monohydrate in the presence of glutamic acid taken in the concentration $C = 10^{-2}$ M begins only at the supersaturation $\gamma = 10$. Thus, the inhibitory effect of glutamic acid is comparable with that exerted by the background electrolyte components and, moreover, tends to increase with increasing number of carboxy groups, as shown by our experiments. The inhibitory effect exerted by the amino acids on crystallization of calcium oxalate monohydrate increases as follows: glycine < alanine < proline < aspartic acid < glutamic acid.

Thus, a strong affinity of dicarboxy groups for calcium oxalate suggests that proteins rich in aspartic and glutamic acids can, on the one hand, suppress the growth of whewellite crystals via adsorption on their surface and, on the other hand, act as nucleation sites via removing calcium ions from solution, i.e., promote formation of calculi. The inhibitory effect of the amino acids is comparable with the exposure to the background electrolyte components but is weaker than that exerted by magnesium cations.

Also, dispersion analysis showed that, upon addition of hydroxyapatite crystals (8.29±0.16 μm) into a calcium oxalate solution containing a glutamic acid addition in the concentration $C = 10^{-2}$ M at $\gamma = 7$ (i.e., under crystallization inhibition conditions), crystallization of oxalate monohydrate takes place and the average size of the solid phase particles increases to 19.14 ± 0.29 μm. Hence, in the presence of hydroxyapatite crystals, formation and growth of whewellite crystals occur even at high amino acid concentrations.

Effect of Amino Acids on Apatite Crystallization

We examined how amino acids affect the electrokinetic properties of the sol particles of stoichiometric and nonstoichiometric (Ca/P = 1.58) hydroxyapatites (Table 4). In our experiments we used amino acids whose content in phosphate type renal calculi and urine is relatively high; pH (6.45±0.05), ionic strength (0.3), and concentration (0.004 M) of the amino acids in the model solutions were close to those in the urolith-forming medium. We found that the sorption of amino acids on crystals of stoichiometric and nonstoichiometric hydroxyapatites proceeds differently, being dependent on the nature of electrostatic interaction. The charge and ξ-potential of the apatite surface depend on the nature of the amino

acid at the indicated concentration, pH, and ionic strength of solution. The interaction of the amino acids with the nonstoichiometric hydroxyapatite crystal surface tends to strengthen with decreasing negative charge of the dominant amino acid in solution. For stoichiometric hydroxyapatite we revealed the inverse dependence.

The strength of electrostatic interaction of the tested amino acids with nonstoichiometric hydroxyapatite decreases as follows: lysine > glycine > glutamic acid > aspartic acid.

For stoichiometric hydroxyapatite with a positively charged surface the strength of electrostatic interaction will display the exactly inverse trend. These trends are probably due to the ability of glycine and lysine for recharging the surface of the nonstoichiometric hydroxyapatite particles, as well as to the change in the sign of the surface charge of stoichiometric hydroxyapatite, associated with adsorption of glycine, aspartic, and glutamic acids.

The particle size distribution curves for apatites, recorded in the presence of different amino acids at the same Ca/P ratio, are similar (although the average particle sizes are different), which suggests that different amino acids interact with basic calcium phosphate by identical mechanisms. Table 4 shows that, throughout the concentration range examined, these acids inhibit the growth of the hydroxyapatite crystals. Specifically, the inhibitory effect of glutamic and aspartic acids tends to increase with increasing Ca/P ratio, as evident from the change in the average size of the corresponding solid phase particles. The revealed trend may be explained by enhancement of electrostatic interaction between the solid phase and amino acids because of variation in the surface charge of the hydroxylapatite particles with the degree of the nonstoichiometry. The electrostatic interaction of the amino acids with the nonstoichiometric hydroxyapatite crystal surface tends to enhance with decreasing negative charge of the dominant form of the amino acid in solution.

The effect of glycine on crystallization of stoichiometric hydroxyapatite is somewhat different from those exerted by the other acids tested. At the initial Ca^{2+}/PO_4^{3-} ratio in solution of 1.90, glycine taken in the concentration of 0.004 M causes an increase in the average particle size relative to the phase obtained in the absence of the amino acids. In the case of different initial Ca^{2+}/PO_4^{3-} ratios in solution, 1.80 and 1.67, the average size of the apatite particles decreased relative to the control samples, though to a lesser extent than in the presence of the other acids tested. Presumably, an increase in the average particle size of the synthesized hydroxyapatite, observed in the presence of glycine, is associated with the ability of the anionic form of glycine for substitution of the hydroxy ions in hydroxyapatite. The inhibitory effect exerted by the amino acids on the growth and aggregation of the hydroxyapatite crystals tends to decrease with increasing ionic strength. This confirms the existence of primarily electrostatic interaction between the examined solid phase and the amino acids. Weakening of adsorption of amino acids on the surface of hydroxyapatite may be associated with sorption of indifferent electrolyte ions.

Thus, the amino acids inhibit the growth of calcium oxalate and phosphate crystals via adsorption on the surface of the growing crystal; the inhibitory effect tends to decrease with increasing ionic strength of solution. The kinetic parameters of the whewellite and hydroxyapatite crystallization depend on the nature and concentration of the amino acid. The strength of the electrostatic interaction of the amino acids (glycine, lysine, and glutamic and aspartic acids) with apatite depends on the degree of nonstoichiometry of the composition of the latter.

CONCLUSIONS

An integrated approach to studying the pathogenic mineral formation in human body was developed and practically applied. It is based on comprehensive examination of the organomineral aggregates (renal, biliary, dental, and salivary calculi) and of the corresponding stone-forming media, as well as on theoretical and experimental modeling in prototypes of biological fluids. A representative collection of renal, biliary, dental, and salivary calculi was thoroughly examined (in terms of morphology, structure, and mineral and chemical compositions); connections between the OMA components were identified; and the ontogenetic features of organomineral aggregates were analyzed. The bile and oral fluid parameters in norm and pathology were determined; the differences in the compositions of pathogenic stone-forming media were revealed; and correlations between the characteristics of the physiological media and of the calculi formed therein were established. The phase formation conditions in urine and oral fluid were examined, and the specific features of crystallization of

the main pathogenic phases of renal calculi (oxalates, phosphate) were determined.

ACKNOWLEDGMENTS

This work was financially supported in part by the Russian Foundation for Basic Research (project no. 10-05-00881-a).

REFERENCES

1. Korago, A.A., *Vvedenie v biomineralogiyu* (Introduction to Biomineralogy), St. Petersburg: Nedra, 1992.
2. Yushkin, N.P., *Singenez, vzaimodeistvie i koevolyutsiya mineral'nogo i zhivogo mirov. Mineralogiya i zhizn'* (Syngenesis, Interaction, and Coevolution of Mineral and Living Worlds: Mineralogy and Life), Syktyvkar, 1993, pp. 5–7.
3. Katkov, V.I., *Mochevye kamni: mineralogiya i genesis* (Uroliths: Mineralogy and Genesis), Syktyvkar: Komi Nauchn. Tsentr Ural. Otd. Ross. Akad. Nauk, 1996.
4. Polienko, A.K., *Cand. Sci. (Geol.-Miner.) Dissertation*, Leningrad, 1986.
5. Tiktinskii, O.L. and Aleksandrov, V.P., *Moche-kamennaya bolezn'* (Urolithiasis), St. Petersburg: Meditsina, 2000.
6. Pal'chik, T.A., Moroz, T.N., Leonova, I.V., and Miroshnichenko, L.V., *Mineraloobrazovanie v organizme cheloveka: Biokosnye vzaimodeistviya: zhizn' i kamen'* (Mineral Formation in Human Body: Bio-Inert Interactions: Life and Rocks), Proc. II Int. Symp., St. Petersburg, Miner. O–vo. Ross. Akad. Nauk, 2004, pp. 186–189.
7. Potapov, S.S., Moroz, T.N., and Kostrovskii, V.G., *Ural Geol. Zh*., 2002, no. 4 (28), pp. 239–244.
8. Sokol, E.V., Nigmatulina, E.N., and Maksimova, N.V., *Khim. Inter. Ust. Razv*., 2003, no. 11, pp. 547–558.
9. Bilobrov, V.M. and Bogdan, N.M., *Osobennosti nornal'nykh i patologicheskikh biomineralov: Mineralogiya i zhizn'* (Features of Normal and Pathological Biominerals: Mineralogy and Life), Materialy mezhgosudrstvennogo mineralogicheskogo seminara (Proc. Int. Mineralog. Seminar), Syktyvkar, 1993, pp. 52–54.
10. Lonsdale, K. and Sutor, D.J., *Kristallografiya*, 1971, vol. 16, no. 6, pp. 1210–1219.
11. Lowenstam, H.A. and Weiner, Sh., *On the Biomineralization*, New York: Oxford Univ. Press, 1989, p. 324.
12. Wandt, M.A.E. and Underhill, L.G., *Br. J. Urol*., 1988, vol. 61, no. 6, p. 474–481.
13. Kodati, V.R. et al., *Applied Spectrosc*., 1990, vol. 44, no. 7, pp. 1134–1136.
14. Haugbert, J.C., Zawacki, S.J., and Nancollas, G.H., *J. Cryst. Growth*, 1983, no. 63, pp. 83–90.
15. Stanford, J.W., *Dental Res*., 1966, vol. 45, no. 1, pp. 128–135.
16. Tas, A.C., *Biomaterials*, 2000, no. 21, pp. 1429–1438.
17. Zhu, P.X., Masuda, Y., and Koumoto, K., *J. Colloid Interface Sci*., 2001, no. 243, pp. 31–36.
18. Kadurin, S.V., *Cand. Sci. (Geol.) Dissertation*, Lviv, 2001.
19. Zuzuk, F.V., *Khim. Inter. Ust. Razv*., 2002, no. 10, pp. 281–295.
20. Golovanova, O.A., Pal'chik, N.A., Berezina N.Yu., and Yudina, L.N., *Khim. Inter. Ust. Razv*., 2006, no. 14, pp. 125–131.
21. Kurkin, B., *"Komsomolskaya Pravda" in Omsk*, July 5, 2002.
22. Golovanova, O.A., Bel'skaya L.V., Lomiashvili, L.M., and Borisenko, M.A., *The Decision to Grant a Patent for Application* no. 2666110490/15(011425) of March 21, 2007.
23. *Biokhimiya* (Biochemistry), Severin, E.S., Ed., Moscow: GEOTAR Med., 2003.
24. Borbat, V.F., Golovanova, O.A., Pyatanova, P.A., and Rosseeva, E.V., RF Patent 2238549. *The Decision to Grant a Patent for Application* no. 2003104252/15 (004438) of February 12, 2003.